

N 7 1 - 3 1 2 8 3

**NASA TECHNICAL  
MEMORANDUM**

NASA TM X-67875

NASA TM X-67875

**CASE FILE  
COPY**

**$^{123}\text{I}$  PRODUCTION FOR USE IN NUCLEAR MEDICINE  
BY SPALLATION OF XENON**

by J. W. Blue and W. K. Roberts  
Lewis Research Center  
Cleveland, Ohio

and

V. J. Sodd and K. L. Scholz  
U. S. Public Health Service  
National Center for Radiological Health  
Cincinnati, Ohio

TECHNICAL PAPER proposed for presentation at  
First Scientific Assembly of the World Federation of Nuclear  
Medicine and Biology  
Los Angeles, California, June 27, 1971

$^{123}\text{I}$  Production For Use In Nuclear Medicine  
by Spallation of Xenon

by

J. W. Blue, V. J. Sodd\*, K. L. Scholz\*, and  
W. K. Roberts

Lewis Research Center  
National Aeronautics and Space Administration  
Cleveland, Ohio

A recent Stanford Institute study estimates that in more than one-half of the nuclear medical procedures, radioiodine is used. A program sponsored by the Public Health Service has shown that  $^{123}\text{I}$  is the best radioiodine from the standpoint of quality of scans and minimization of patient dose. If  $^{123}\text{I}$  is to replace  $^{131}\text{I}$  the problem of production of large quantities must be solved. Dr. Stang of Brookhaven and Dr. O'Brien of LASL have suggested that the new generation of high current and high energy proton accelerators can produce large quantities of many isotopes.

The present study is directed towards a specific means of  $^{123}\text{I}$  production by this new generation of accelerators. The First Slide shows a method of  $^{123}\text{I}$  production that we developed several years ago for low energy cyclotrons. Dr. Sodd will discuss the current status of this development in another paper at the annual meeting of the Society of Nuclear Medicine. The approximate rate of  $^{123}\text{I}$  production by this method is sufficient for five to ten patients per hour depending on the procedure, clearly inadequate for widespread use of radioiodine. To review, the basic method is to produce  $^{123}\text{Xe}$  which is swept out of the target material by a slow flow of helium gas. The radioiodine impurities are trapped at dry ice temperature while the  $^{123}\text{Xe}$  is trapped at liquid nitrogen temperature. The  $^{123}\text{Xe}$  is subsequently allowed to decay to  $^{123}\text{I}$ . The method studied in this paper is shown in the lower part of the slide and you can see that the essential idea is the same. In this case  $^{123}\text{Xe}$  is produced by the so-called spallation reactions. Along with the desired  $^{123}\text{Xe}$ , a host of radioimpurities are produced. The present study had the objectives of 1) to determine the yield of  $^{123}\text{Xe}$  at several energies; 2) to determine the applicability

---

\*Public Health Service, National Center for Radiological  
Health, Cincinnati, Ohio

in this situation of the physical separation method used with the tellurium target and 3) to determine the yield of  $^{125}\text{Xe}$  which cannot be separated from the  $^{123}\text{Xe}$  by a simple method.  $^{125}\text{Xe}$  leads to  $^{125}\text{I}$  by decay which in turn emits gamma rays of too low energy to interfere with scintograms but does contribute to patient radiation dose.

Two experiments were carried out at the Space Radiation Effects Laboratory cyclotron (SREL). Slide 2 shows schematically the first experimental arrangement in which a cylindrical aluminum tank 1 was filled with natural xenon gas and bombarded with protons at one of the three energies indicated. Aluminum monitor foils were used to monitor the number of incident protons during the one-half hour bombardment at a current about 50 nanoamperes. After the bombardment V-1 was opened and the xenon gas in tank 1 was allowed to expand into tank 2. Since the two tanks were the same size, half of the  $^{123}\text{Xe}$  produced during the bombardment was transferred to tank 2 which was subsequently disconnected from the radioactive tank 1. Then the intensity of the 148 keV gamma ray from  $^{123}\text{Xe}$  could be determined. Slide 3 shows the steps followed. The amount of  $^{123}\text{I}$  produced was determined by counting a leach of tank 2 in a geometry that had been calibrated. The cross section in millibarns for  $^{123}\text{Xe}$  production is given in Slide 4. Also shown is the calculated amount of  $^{123}\text{I}$  produced in a one hour of bombardment at 1 ma of beam which is consistent with the output of the high intensity machines.

Due to electronic problems, the yield of  $^{125}\text{Xe}$  could not be determined from this first experiment. The experiment was repeated in an arrangement shown in Slide 5. The target chamber is wider in diameter and not so long. This was done because at the lowest energy, the beam was divergent enough so that some protons that entered the front surface of the can came out through the side wall. This made the determination of the path length in the gas uncertain. Shortly after the bombardment (15 min. at 50 nanoamperes) all the gas in tank 1 was removed to tank 2 by cryopumping; that is, V1 was opened and tank 2 immersed in liquid nitrogen. After a period long compared to the 2 hour half-life of  $^{123}\text{Xe}$  elapsed, the spectrum of tank 2 was obtained. This is shown in Slide 6 along with the spectrum of the same tank 2 after the xenon had been removed cryopumping 2 and also the spectrum of the leachate of tank 2. It is clear that while  $^{123}\text{I}$  has the dominant gamma ray there are many radioimpurities. The most prominent is  $^{111}\text{In}$ , which was separated from the iodine by

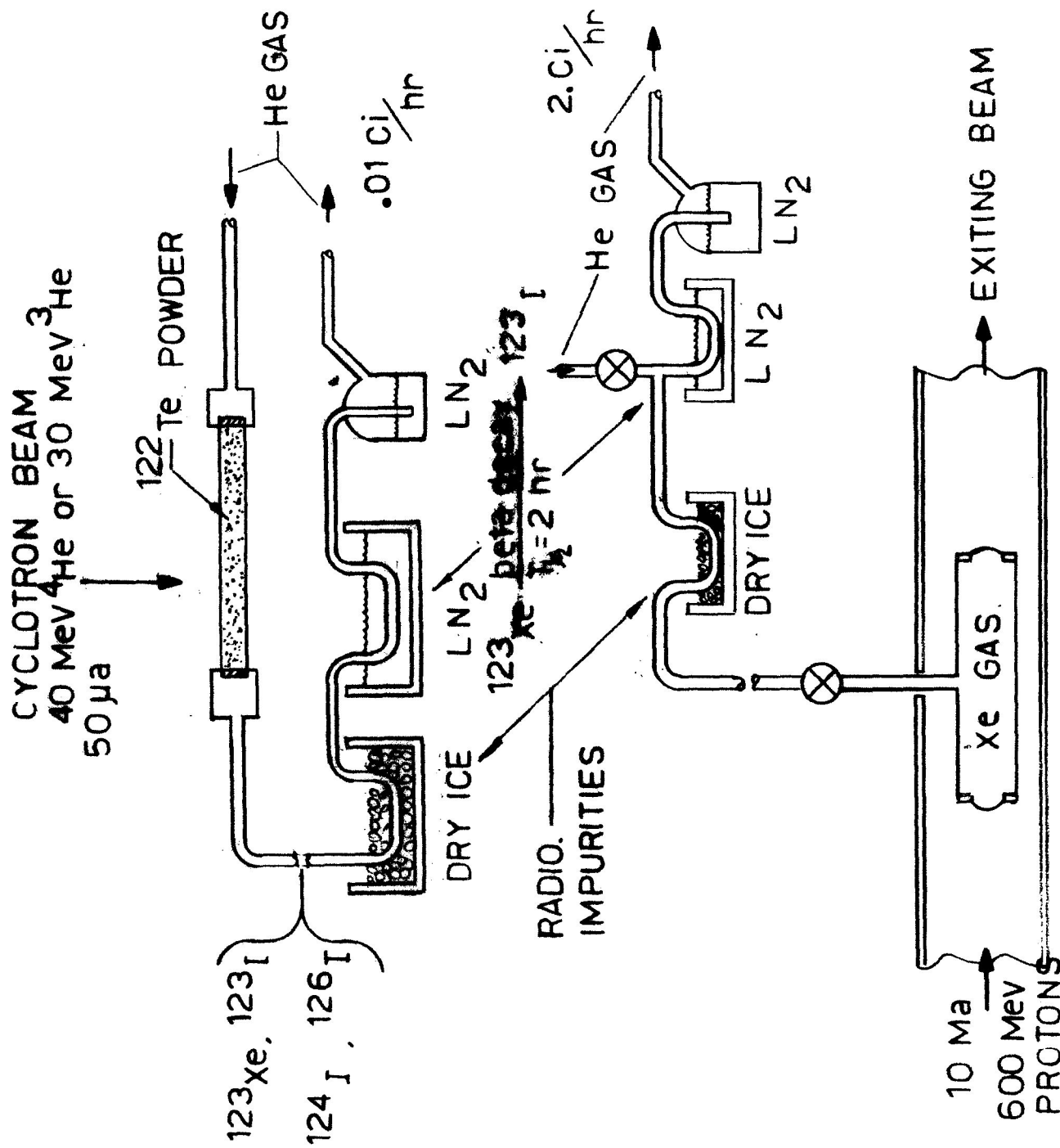
adding ferric chloride and coprecipitating with hydroxide. Slide 7 shows the spectra of the precipitate and the filtrate. The impurities were more easily identified since the indium and tellurium activities were exclusively in the precipitate and the iodine, cesium and antimony were in the filtrate.

In another irradiation a trap at dry ice temperature was inserted between tanks 1 and 2 as shown in Slide 8. The resulting bombardment produced the spectrum shown at the top of Slide 9 of the trap, containing tellurium, iodine, indium, and antimony activities. The leachate of tank 2 shown in the lower spectrum now shows considerably fewer contaminants and it is clear that an additional chemical separation as the OH coprecipitation with  $\text{Fe}(\text{OH})_3$  would remove most of the remaining contaminants. However, we feel that the wet chemical step is not necessary since the dry ice trap has not been studied and could be improved.

The last slide (Slide 10) shows the details of the target assembly as it would sit in the accelerator beam duct. In this chamber, xenon gas at a pressure of 5 atmospheres would absorb energy at a rate of about 2 kw. About 30% would reach the water cooled walls as electromagnetic radiation. The remainder would heat the gas and cause convection as shown in the lower part of the slide. Finned walls improve the heat transfer from the gas. Beryllium is the ideal window material but aluminum would also be satisfactory. The windows would extend the life by keeping the temperature down.

We believe a xenon gas target for  $^{123}\text{I}$  production has the following advantages.

- 1) Simplicity
- 2) The target can be handled remotely as by cryopumping and thus minimizes radiation exposure to operating personnel.
- 3) Tagging of pharmaceuticals can be easily done by cryopumping the irradiated gas into a vessel containing the pharmaceutical. We have tagged hippuran in this manner and achieved better than 40% efficiency.
- 4) Cooling of the target is readily accomplished. This is a problem in solid targets particularly if the thermal conductivity is low.
- 5) Inexpensive in that the same target materials can be reused.



CS-59148

Fig. 1

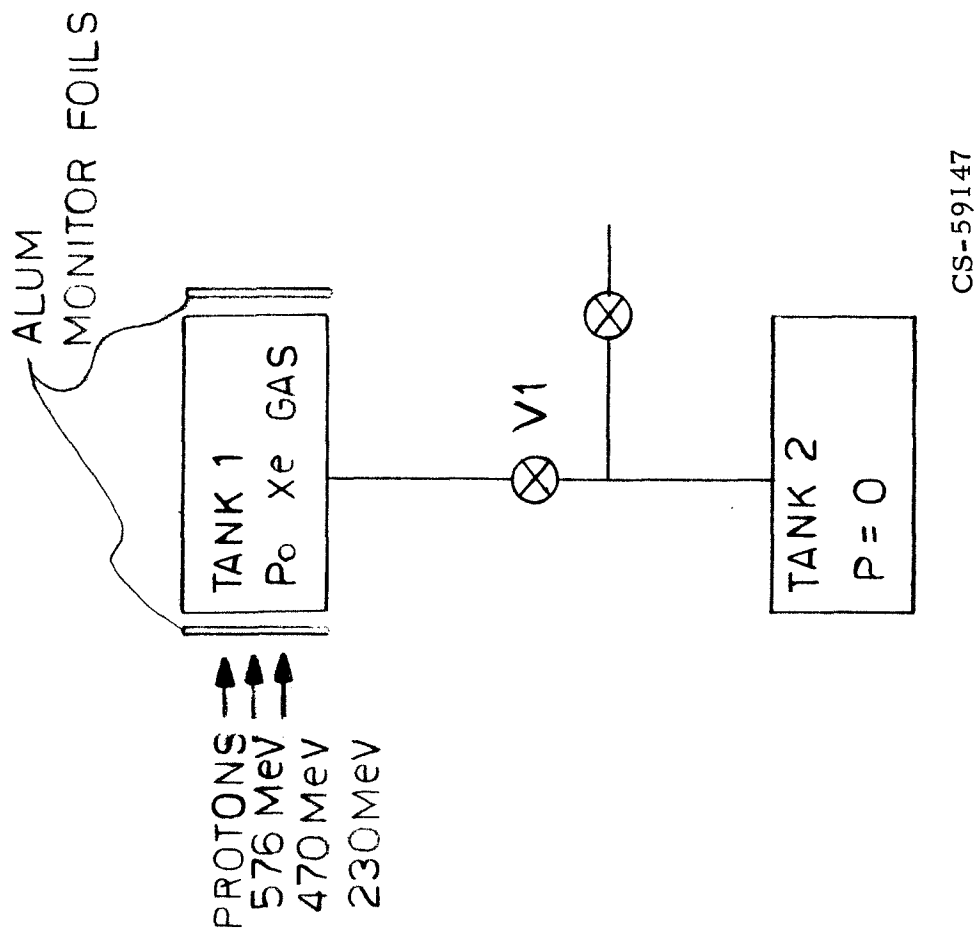
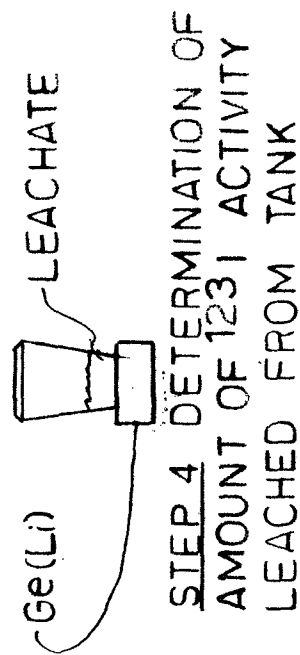
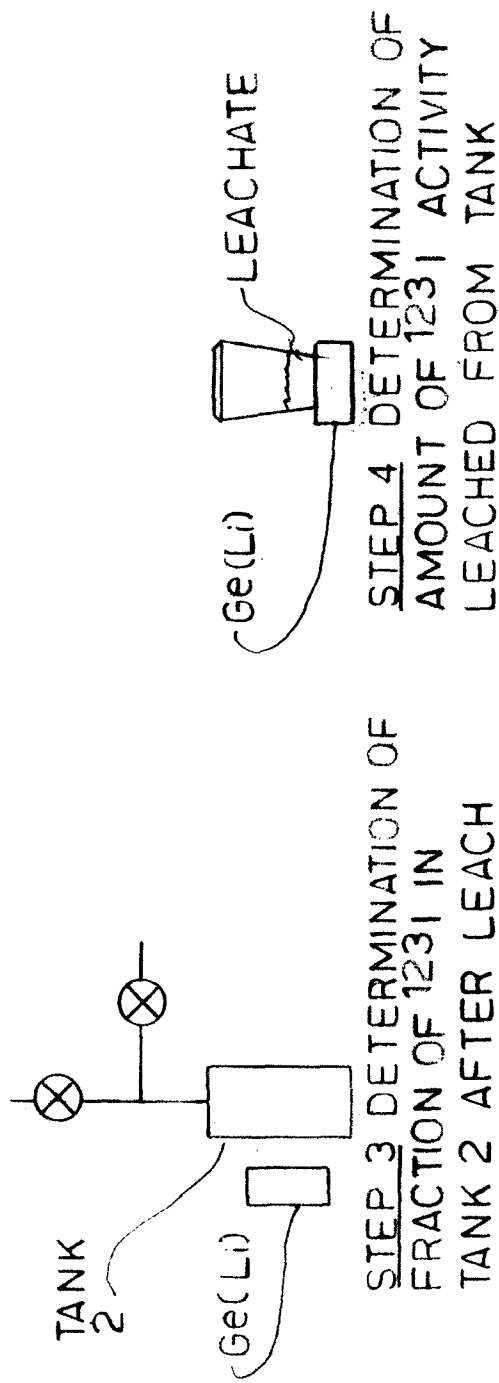
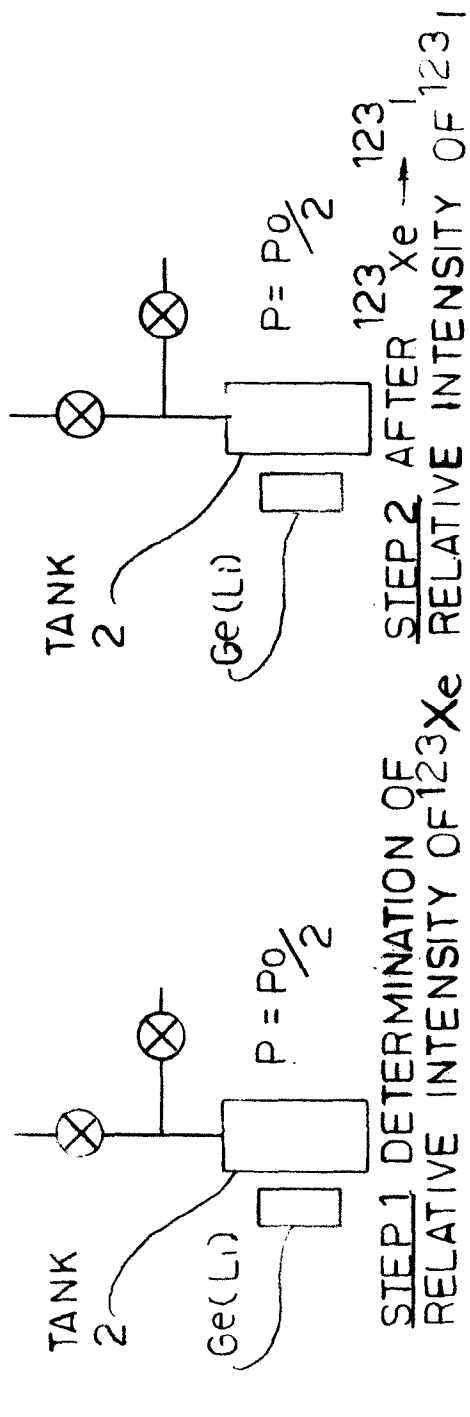


Fig. 2



CS-59149

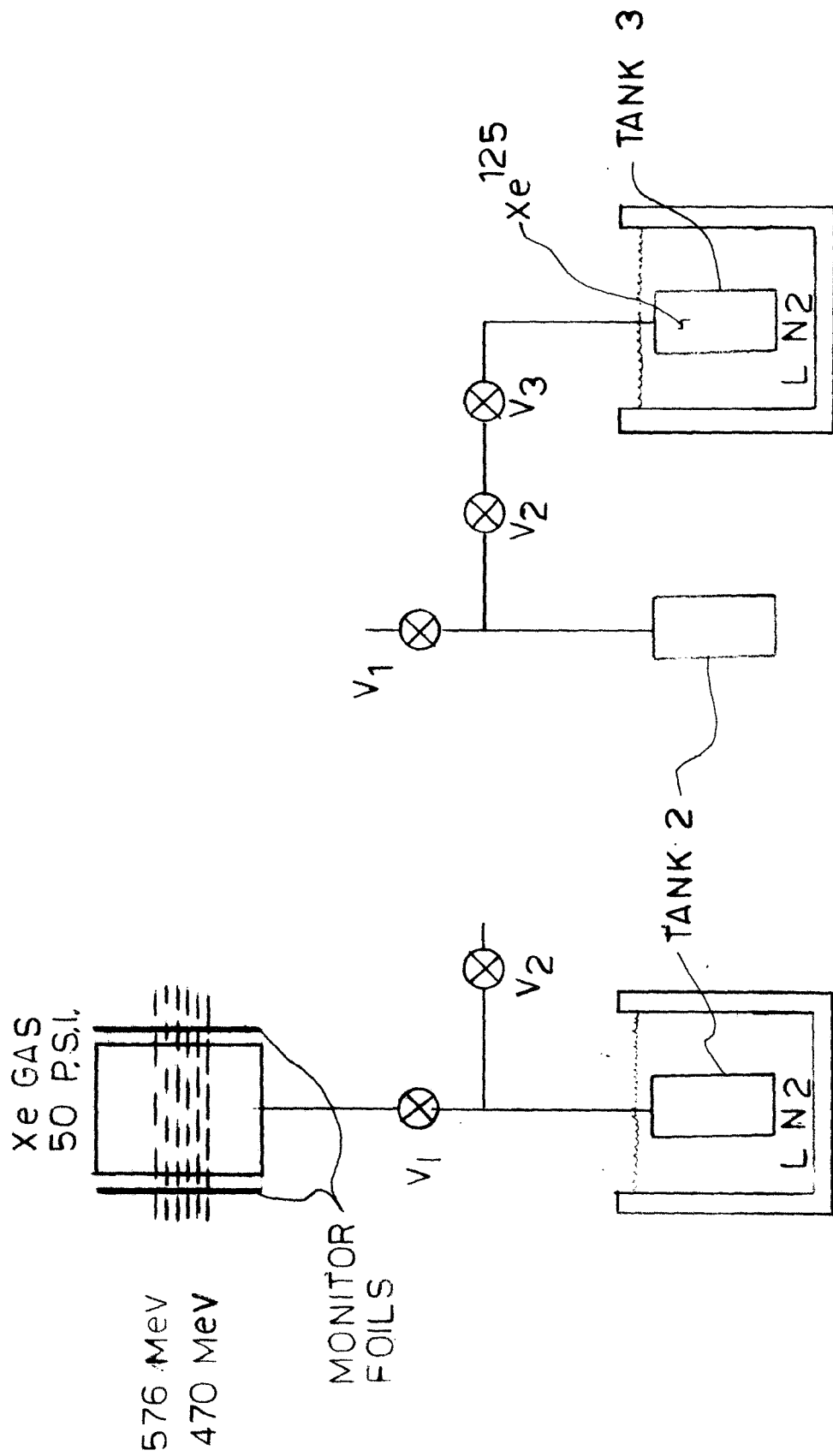
Fig. 3

# RESULTS OF $^{123}\text{Xe}$ CROSS SECTION MEASUREMENT

PROTON ENERGY, MeV	$^{123}\text{Xe}$ CROSS SECTION, mb	MAXIMUM CALCULATED YIELD OF $^{123}\text{I}$ , Ci/HR
576	37	1.3
470	50	1.8
230	22	.8

Fig. 4





STEP 1

STEP 2

CS-59150

Fig. 5

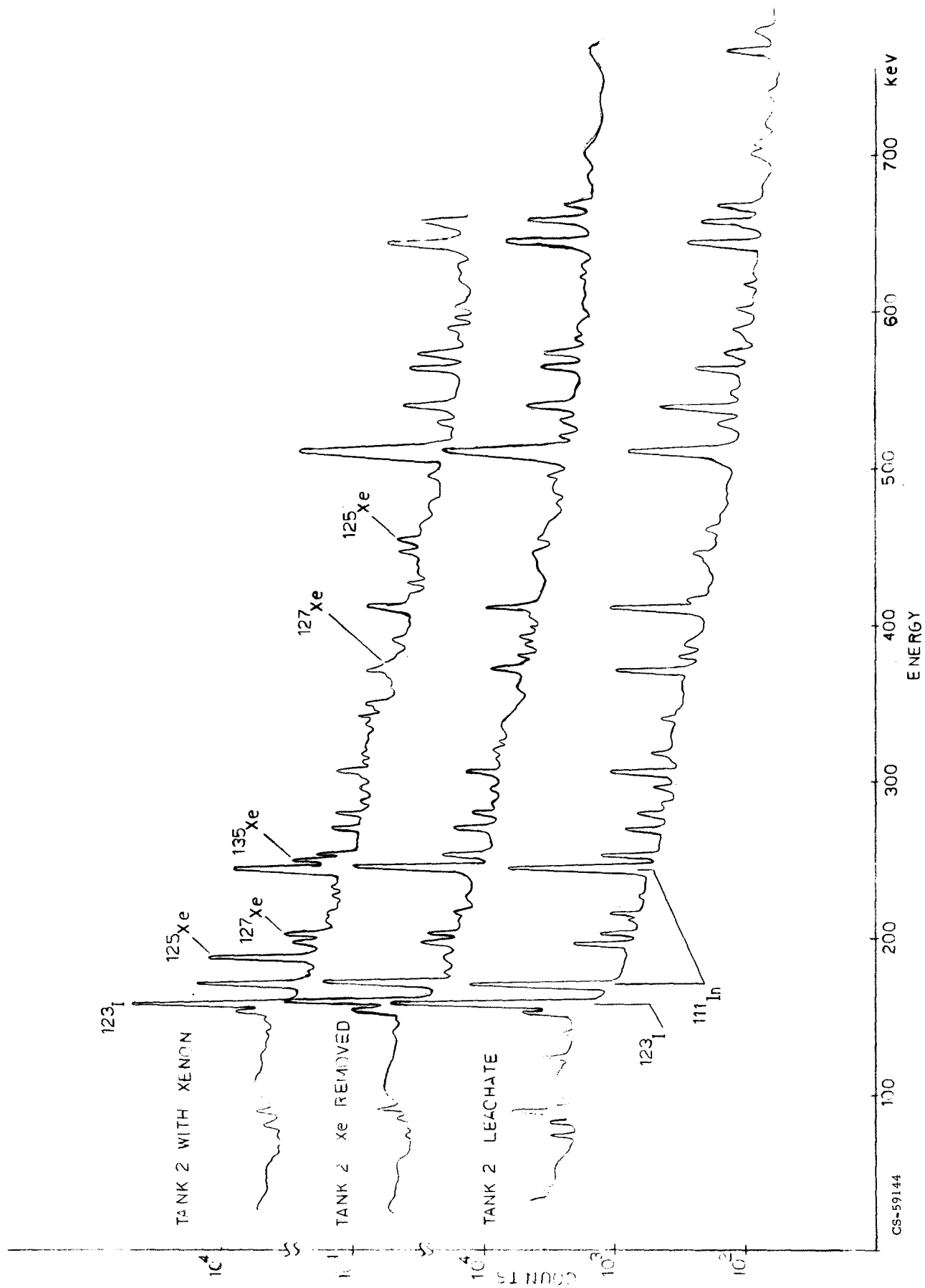


Fig. 6

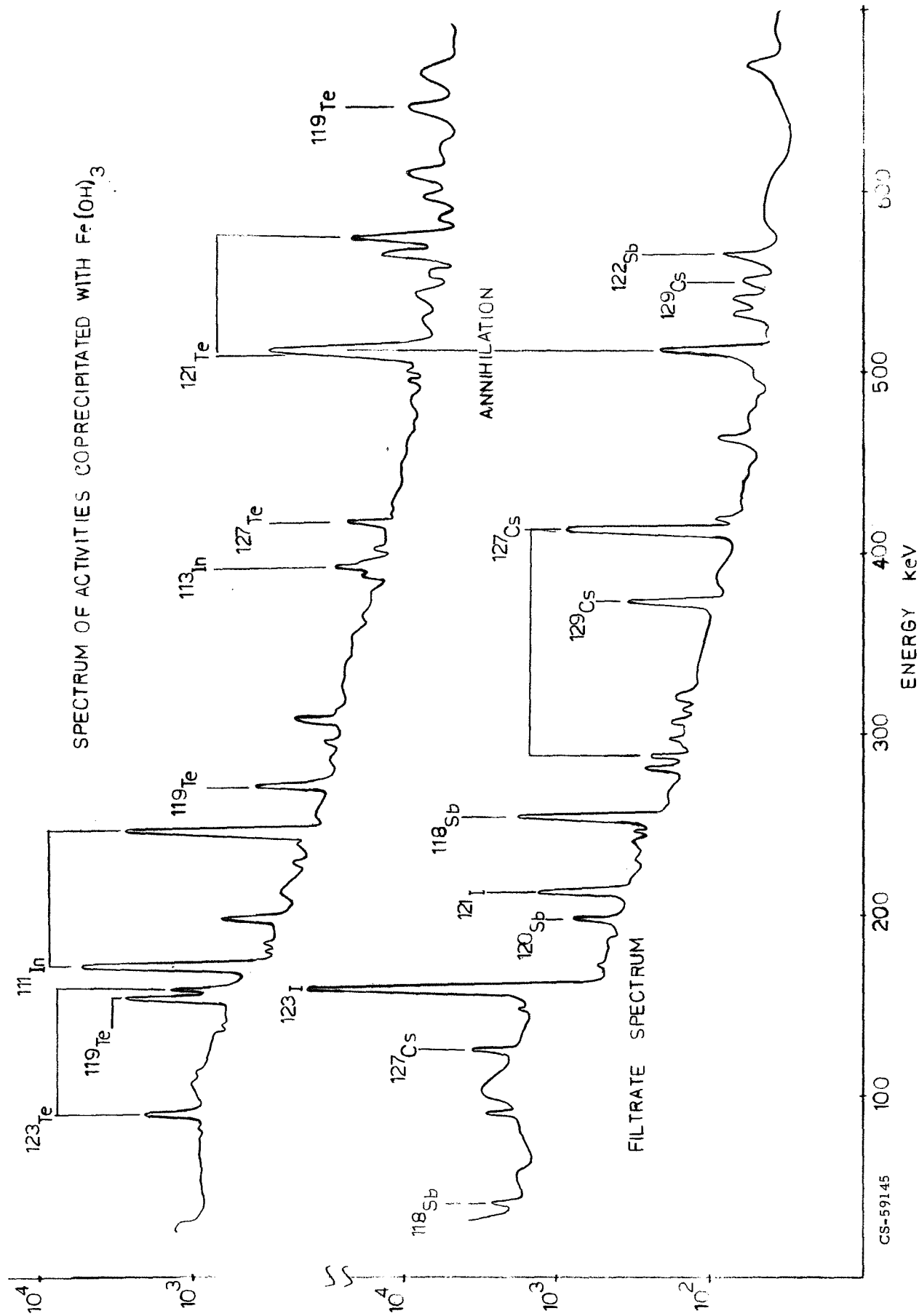
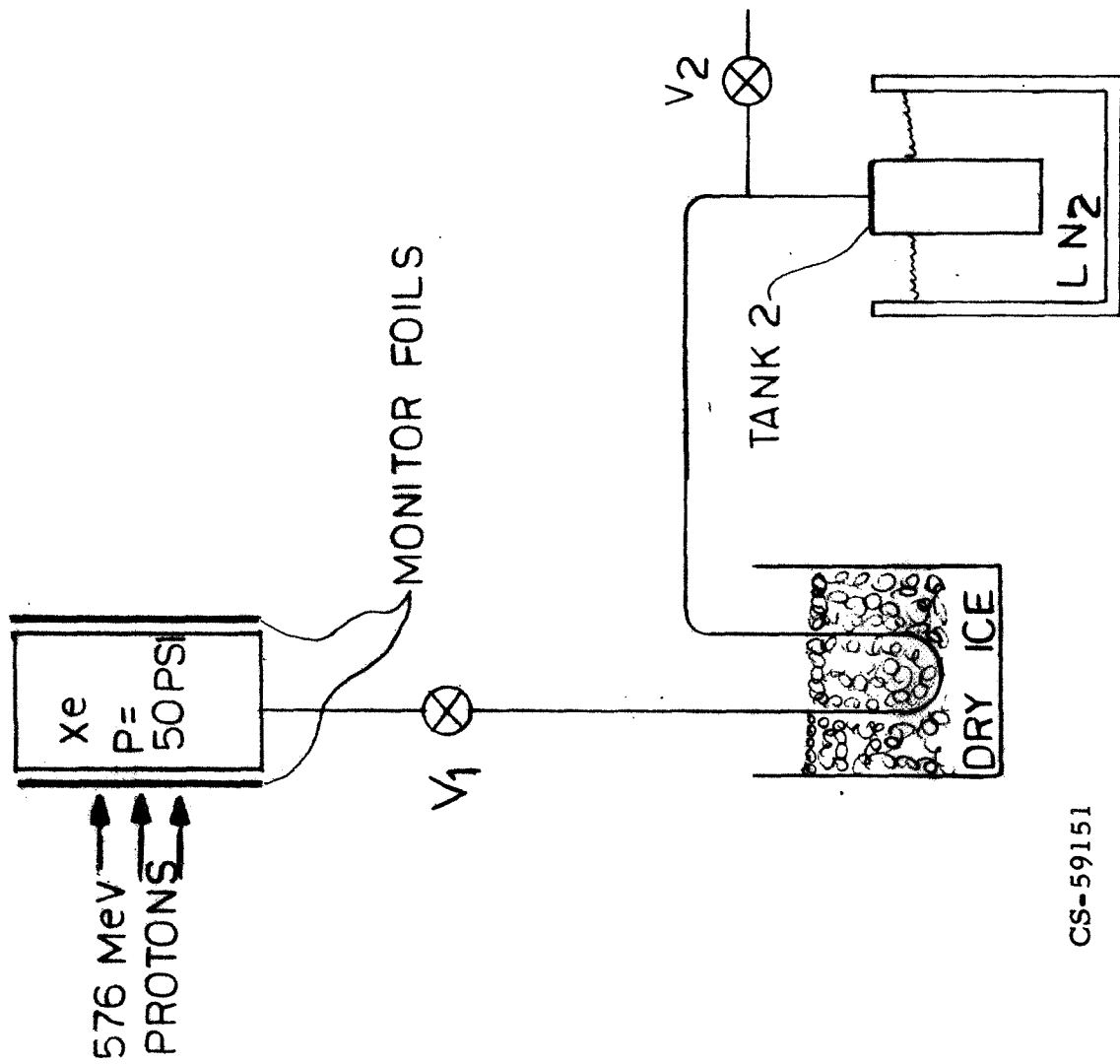


Fig. 7



CS-59151

Fig. 8

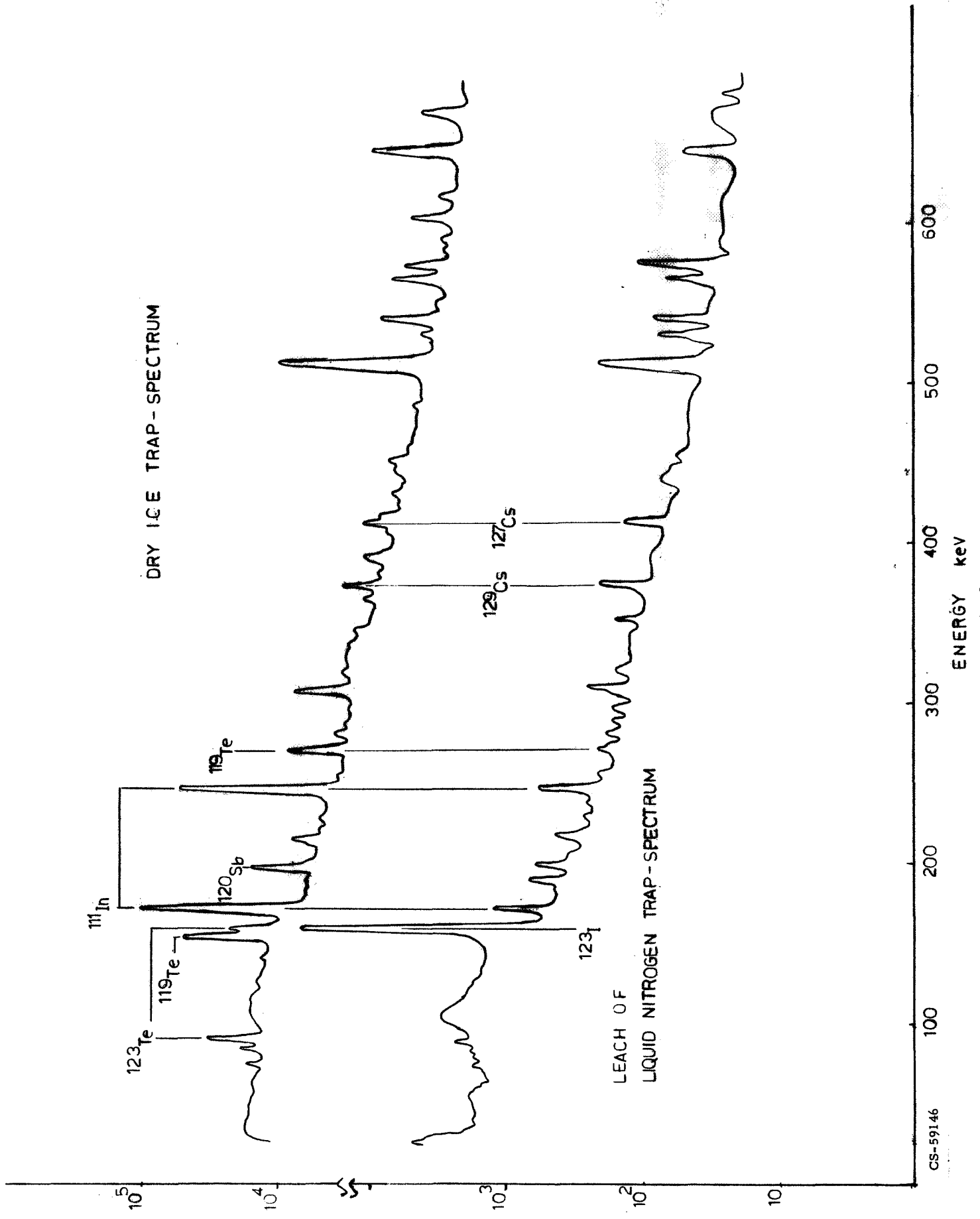


Fig. 9

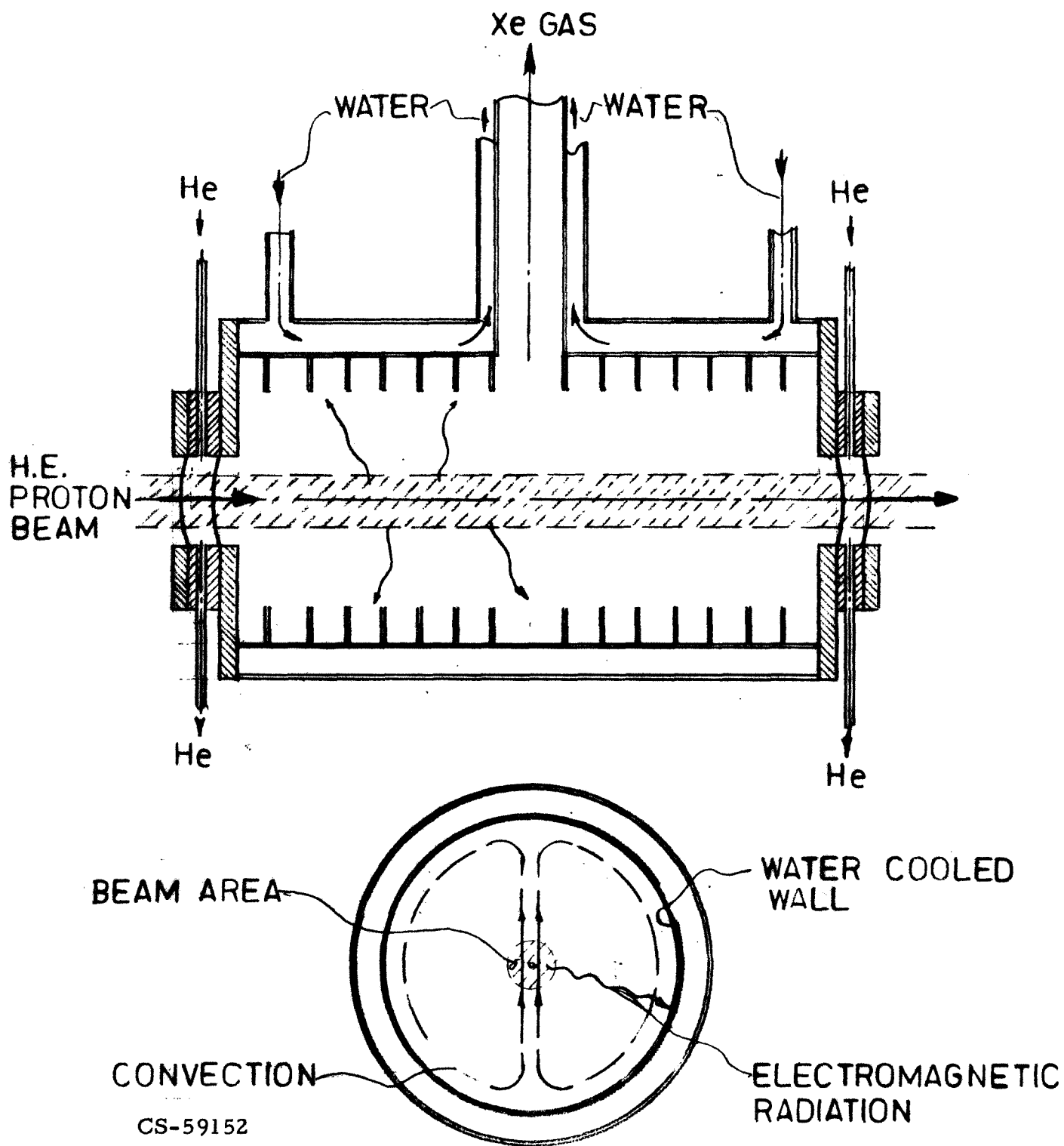


Fig. 10